

# Preparation and Characterization of Hydroxyapatite/Chitosan–Gelatin Network Composite

YU JI YIN,<sup>1</sup> FENG ZHAO,<sup>1</sup> XUE FENG SONG,<sup>1</sup> KANG DE YAO,<sup>1</sup> WILLIAM W. LU,<sup>2</sup> J. CHIYAN LEONG<sup>2</sup>

<sup>1</sup> Research Institute of Polymeric Materials, Tianjin University, Tianjin 300072, People's Republic of China

<sup>2</sup> Department of Orthopedic Surgery, Queen Mary Hospital, University of Hong Kong, Hong Kong, People's Republic of China

Received 26 May 1999; accepted 10 September 1999

**ABSTRACT:** A novel composite composed of hydroxyapatite (HA) and a network formed via cocrosslinking of chitosan and gelatin with glutaraldehyde was developed. Two preparation methods are described in detail. A porous material, with similar organic–inorganic constituents to that of natural bone, was made by a unique sol–gel method. The formation of the network in the presence of HA was characterized using IR analysis. The morphology of the composites was also examined using SEM. In addition, XRD was applied to estimate the change in the component crystal. The results indicate that the presence of HA does not retard the formation of the chitosan/gelatin network. On the other hand, the polymer matrix has hardly any influence on the high crystallinity of HA. © 2000 John Wiley & Sons, Inc. *J Appl Polym Sci* 77: 2929–2938, 2000

**Key words:** chitosan/gelatin network; hydroxyapatite; composite

## INTRODUCTION

As the consequence of tumors, infections, trauma, or other causes, bone defects need to be repaired. An ideal clinical bone substitute should not only be nontoxic, biocompatible with all the tissues, including bone and blood, around it, and osteoconductive to form a good vicinity in the interface of nature bone and the implant, but also maintain good mechanical properties in the wet state. Nor is that all: Another vital function of the implant is to be osteoinductive, which means that the bone cells migrate toward and inside the implant to replace it by induced cells and to fill the cavity with natural bone.<sup>1</sup>

Hydroxyapatite [HA:  $\text{Ca}_{10}(\text{PO}_4)_6(\text{OH})_2$ ],<sup>2,3</sup> which has been proved to possess good properties of

ideal hardness, biocompatibility, osteoconductivity, a certain degree of bioactivity, and high resistance to moisture, has been used in a variety of oral and maxillofacial applications. It is available in dense blocks, porous blocks, and granules. However, each of these forms has its own drawbacks: Dense HA is difficult to machine without causing large-scale fracture, granules tend to migrate, and the macroporous material leaves a ragged surface finish.<sup>4</sup> Therefore, in recent years, HA-reinforced degradable polymers, such as collagen,<sup>5–11</sup> gelatin,<sup>12–14</sup> chitosan,<sup>15–17</sup> chitin,<sup>18</sup> a block copolymer of poly(ethylene glycol) and poly(butylene terephthalate) (PEG/PBT),<sup>19</sup> polyhydroxybutyrate (PHB),<sup>20</sup> and polylactide (PLA),<sup>21–23</sup> have been developed to fix bone fractures. When the polymer matrix is reabsorbed, new bone may intergrow around the HA particles.

Gelatin is a protein made soluble by hydrolysis of collagen derived from the skin, white connective tissue, and bones of animals. It has many attractive properties such as nonantigenicity, bio-

Correspondence to: K. D. Yao.  
Contract grant sponsor: National Science Foundation of China; contract grant number: 59883002.

*Journal of Applied Polymer Science*, Vol. 77, 2929–2938 (2000)  
© 2000 John Wiley & Sons, Inc.

compatibility, plasticity, and adhesiveness. In recent years, research also focused on composites composed of gelatin and apatite. Formaldehyde-crosslinked gelatin and tricalcium phosphate (GTF)<sup>24</sup> was shown to be osteoconductive and bioabsorbable for filling small irregular defects, while glutaraldehyde-crosslinked gelatin and tricalcium phosphate (GTG)<sup>1</sup> was shown to be biologically suitable to repair large bone defects and to promote new bone formation. With the purpose of simulating the formation process of natural bone, several studies<sup>12,25,26</sup> investigated the formation of HA in gelatin gels. It was reported<sup>12</sup> that the formation of HA–gel composites occurs under steady-state pH conditions. The preparation of HA–gelatin composite films with an anisotropic property<sup>13</sup> indicated that the films could be modulated through variation in composition and mechanical deformation in order to obtain biomaterials giving specific mechanical functions.

Chitin is one of the most abundant natural polymers and is available largely in the cuticle of crustaceans such as shrimps and crabs,<sup>27</sup> where, in conjunction with proteins, it acts as a support for inorganic calcite. Anticipated to be analogous to its role as part of the organic matrix in the crustacean integument, a chitin-containing HA composite<sup>18</sup> was developed as a potential hard-tissue substitute material. The composite exhibited a fairly good distribution of HA filler in the chitin matrix, a retention of the plastic properties, and a reduction in strength for the more highly filled composites.

Chitosan is an aminopolysaccharide obtained by deacetylation of chitin. It has been reported to be safe, hemostatic, and osteoconductive and to promote wound healing.<sup>28–30</sup> Thus, chitosan seems to be a suitable biopolymer for use in a wide variety of biomedical applications. A chitosan-bonded HA bone-filling paste<sup>15–17,30</sup> was found to possess neutral pH, short setting time, relatively high compressive strength, and osteoconductive properties, while subperiosteal implantation of the chitosan–HA composite membranes over rat calvaria revealed that the membranes were well tolerated, with fibrous encapsulation and occasional osteogenesis.<sup>31</sup>

Even though many kinds of artificial bone have been investigated, each of them has its own advantages and disadvantages. For the purpose of optimizing properties of HA, a novel bone composite was developed by combining HA with a chitosan–gelatin network.

**Table I** The Feeding Components in Preparing Composites

Mass Ratio of HA (%)	HA (g)	Chitosan Solution (g)	Gelatin (g)	Glutaraldehyde Solution (g)
0	0	14.33	1.0	0.7
10	0.2	12.90	0.9	0.7
20	0.4	11.47	0.8	0.7
30	0.6	10.03	0.7	0.7
40	0.8	8.60	0.6	0.6
50	1.0	7.16	0.5	0.5

## EXPERIMENTAL

### Materials

HA, with an average grain of less than 75  $\mu\text{m}$ , was obtained from the Engineering Research Center in Biomaterials, Sichuan University (Chengdu, China). To minimize the particles, an agate-ball mill was used and the resultant grain size was less than 10  $\mu\text{m}$ .

Chitosan (mean molecular weight  $8.0 \times 10^5$ ) was supplied by the Qingdao Medical Institute (Qingdao, China). It was purified as follows: Chitosan was dissolved in a 2% acetic acid aqueous solution until a homogeneous 1% chitosan solution was attained. The solution was neutralized to pH 9.0 with a 10% NaOH solution to precipitate chitosan, and the chitosan obtained was washed with deionized distilled water and air-dried.

The gelatin powder from bovine skin was provided by the Sigma Chemical Co. (St. Louis, MO). Glutaraldehyde and acetic acid were all chemical grade.

### Preparation of HA/Chitosan–Gelatin Composites

A chitosan sol was prepared by dissolving 3.75 g of chitosan in a solution of 1 g acetic acid in 49 mL deionized distilled water and maintaining it at room temperature for 24 h until the chitosan was entirely dissolved. A glutaraldehyde solution was prepared by dissolving 0.5 mL glutaraldehyde (50%) in 250 mL deionized distilled water.

Composites with different HA content (cf. Table I) were prepared as follows: The sample composed of 30% by mass of HA, 35% of chitosan, and 35% of gelatin is used as an example. First, 0.6 g HA powder was added to 200 mL deionized distilled water, which was then ultrasonicated until the HA powder was thoroughly dispersed in the water. Second, the slurry was held for 5 h to let



**Scheme 1** Crosslinking reactions of glutaraldehyde (GA) with chitosan (CS) and gelatin (Glt).

the HA powder deposit. The deposited HA paste was mingled with a 10.03 g chitosan solution under agitation. Next, 0.7 g gelatin was added to the mixture. After the gelatin was dissolved, a 0.7 g glutaraldehyde aqueous solution was incorporated dropwise into the slurry while stirring. Then, at last, the resulting mixture, with homogeneously dispersed HA powder, was cast into a mold and air-dried to obtain a composite plate.

#### Preparation of Porous HA/Chitosan-Gelatin Network Composites

Gelatin, 1.5 g, was dissolved in a 21.5 g chitosan solution; then, 7 g HA powder was added to the

solution, stirring 10 min to disperse the HA. Next, the mixture was transferred to an agate mortar, and a suitable amount of the glutaraldehyde aqueous solution was added dropwise under manual grinding. The resulting paste was poured into a stainless mold, and the mold was put in a press and kept at 50°C for 0.5 h under a pressure of 20 MPa. When the mold was cooled, the plate was taken out and air-dried.

#### Measurement of Mechanical Properties

The composite plates were cut into the required shape and tested at controlled room temperature ( $23 \pm 1^\circ\text{C}$ ). Six specimens were used in each mechanical test, and the result was an average value.

The impact strength was estimated by using a Dys testing apparatus (Dynstat, Germany). The dimension of the specimens was  $10 \times 4 \times 2$  mm.

The three-point bending test was carried out for the specimens ( $25 \times 4 \times 4$  mm) at room

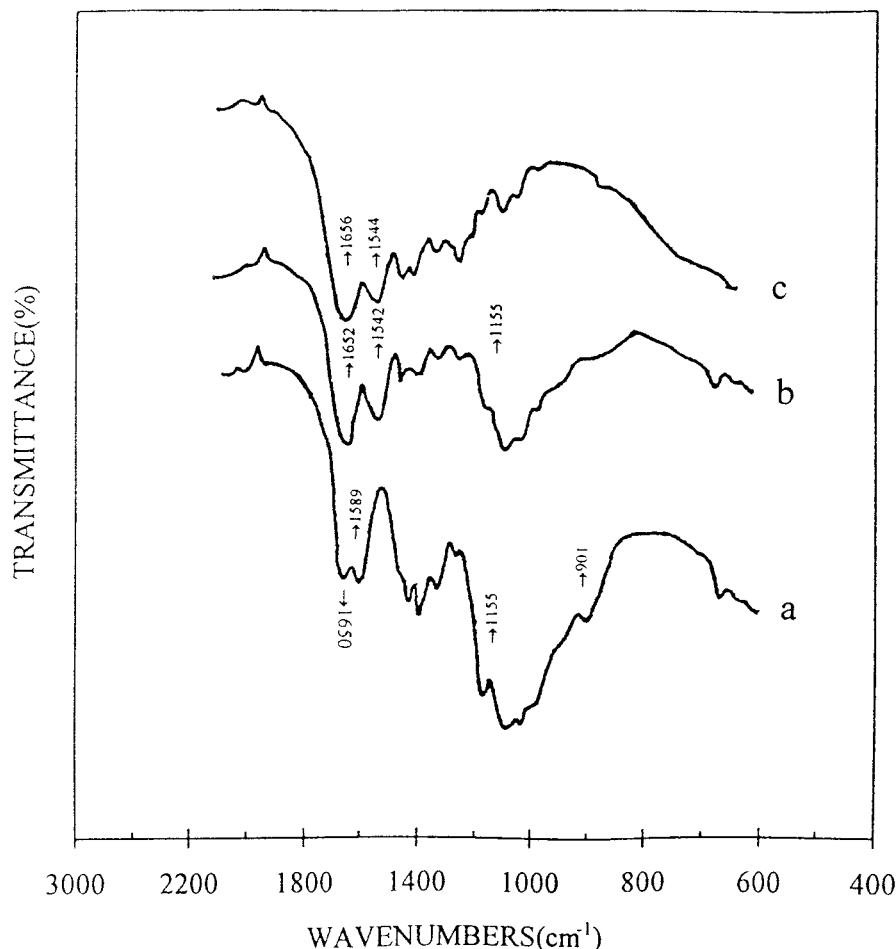


**Figure 1** IR spectra of (a) chitosan, (b) the chitosan/gelatin hybrid polymer network, and (c) gelatin.

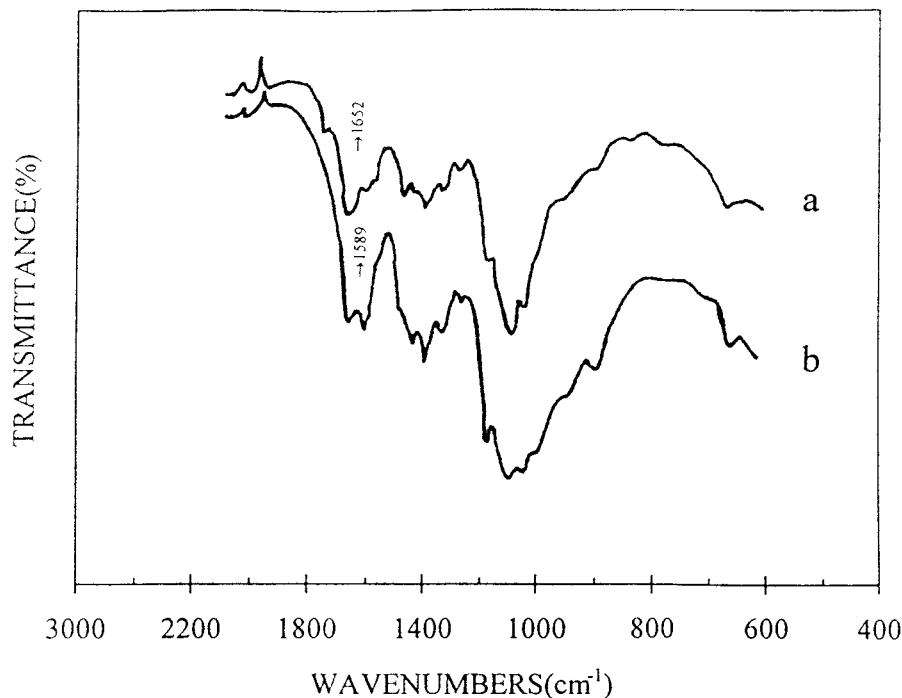


**Figure 2** IR spectra of (a) crosslinked chitosan and (b) chitosan.

temperature. The specimens were tested to failure on an SJ-1A floor standing test machine (Nanjing Electric Automation Instrument Factory, China) at a crosshead speed of  $0.368 \text{ mm min}^{-1}$ .

### IR Spectra

The gelatin was dissolved in the chitosan solution and a 0.5% glutaraldehyde aqueous solution was added dropwise into the mixture under stirring. The mixture was then cast into a plastic-frame mold. After evaporating at  $55 \pm 1^\circ\text{C}$ , a chitosan/gelatin network membrane was formed.

The samples of the composite and network were put in a vacuum oven at  $50^\circ\text{C}$  for 48 h before they were ground to a suitable size for IR analysis with a Nicolet 5DX FTIR spectrometer. Pure chitosan and air-dried gelatin were analyzed as the controls.

### XRD Analysis

The ground samples were characterized by X-ray diffraction (XRD). The patterns were recorded with a 2038 XRD analyzer using  $\text{CuK}\alpha$  radiation ( $\lambda = 1.542 \text{ nm}$ ), generated at 35 kV and 10 mA. The samples were scanned from  $8^\circ$  to  $70^\circ$  in  $2\theta$

(where  $\theta$  is the Bragg angle) in a continuous mode ( $4.0^\circ 2\theta \text{ min}^{-1}$ ) using a strip-chart recorder.

### SEM Observation

For scanning electron microscopy (SEM) observation, the HA particles or the fracture surface of the composite specimen used for measurement were gold-coated, and then SEM observation was carried out with a Hitachi X-650 scanning electron microscope.

## RESULTS AND DISCUSSION

### Composite Formation

The aldehyde groups  $-\text{CHO}$  of glutaraldehyde can react with the amino groups  $-\text{NH}_2$  stemming from chitosan and gelatin. The crosslinking reactions are shown in Scheme 1.

Figure 1 shows the IR spectra of chitosan, gelatin, and the chitosan/gelatin hybrid polymer network. The IR spectrum of chitosan [Fig. 1(a)] displays peaks around  $901$  and  $1155 \text{ cm}^{-1}$ , assigned to the saccharine structure and a weaker amino characteristic peak at  $1589 \text{ cm}^{-1}$ . There is a stronger absorption band at  $1650 \text{ cm}^{-1}$  corresponding

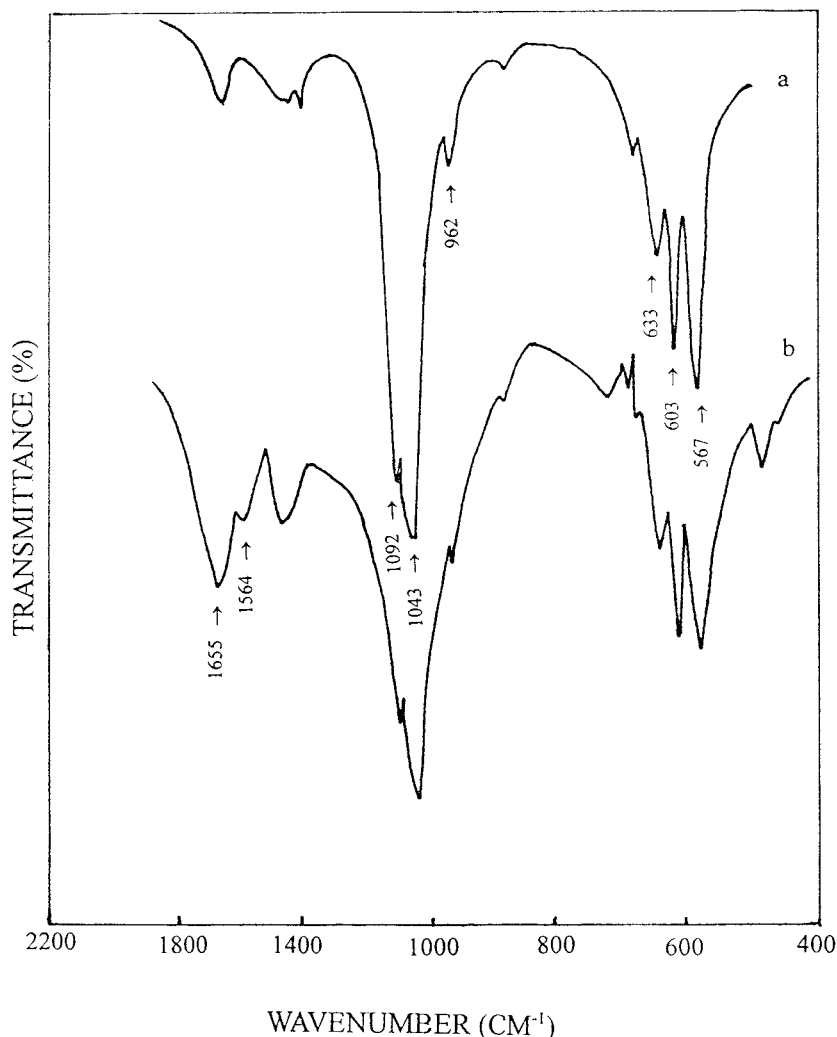


**Figure 3** IR spectra of (a) HA and (b) HA/polymer composite.

to the amide of chitin. The ampholyte gelatin is characterized by its amino band at  $1544\text{ cm}^{-1}$  and a carbonyl peak at  $1656\text{ cm}^{-1}$  [Fig. 1(c)].

The IR spectrum of the chitosan/gelatin hybrid polymer network [Fig. 1(b)] shows significant peaks at  $1542$  and  $1652\text{ cm}^{-1}$ , which are attributed to the characteristics of imine C=N, formed by the crosslinking reactions illustrated in Scheme 1. Hence, it can be confirmed that the hybrid polymer network forms via —C=N— formation due to amino groups reacting with the aldehyde groups of glutaraldehyde. There are hydrogen bonds between chitosan and gelatin within the network.

To prove the mechanism, the IR spectrum of crosslinked chitosan was also tested [Fig. 2(a)]. From the pattern, it can be seen that there is a new absorption band at  $1652\text{ cm}^{-1}$ , while the

band at  $1589\text{ cm}^{-1}$ , which is assigned to amino groups, has disappeared. It is believed that this results from the Schiff base reaction between the amino groups of chitosan and the aldehyde groups of glutaraldehyde.

The IR spectra of the HA and the composite are shown in Figure 3. Figure 3(a) indicates the characteristic features of HA powder prior to the combination with the chitosan/gelatin hybrid polymer network. The intensities of absorption bands at  $1092$ ,  $1043$ ,  $962$ ,  $603$ , and  $567\text{ cm}^{-1}$  are assigned to  $\text{PO}_4$  groups in the HA and  $633\text{ cm}^{-1}$  corresponds to the vibration of —OH. All these bands also exist in the IR spectrum of the composite.

The spectrum of Figure 3(b) shows the characteristic features of the composite. Besides the typical absorption bands of HA, some new bands can be observed in the spectrum. For example, the

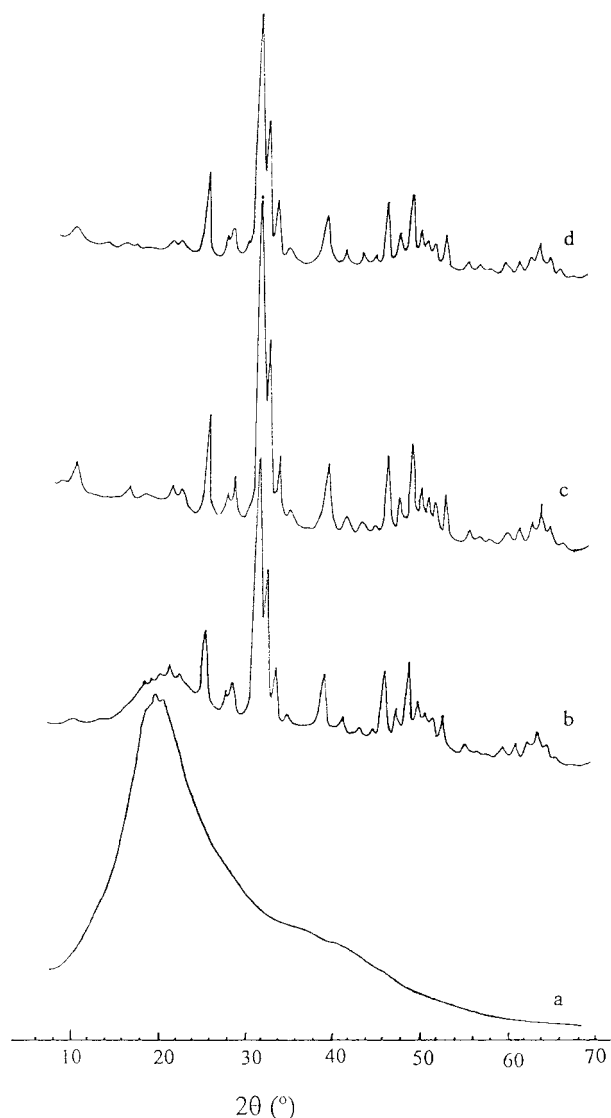


**Figure 4** XRD patterns of the composite with HA content in the range of 0–100 wt %: (a) 0%; (b) 30%; (c) 70%; (d) 100%.

presence of the  $1655\text{ cm}^{-1}$  band is attributed to the stretching mode of the C=N vibration, and the band at  $1564\text{ cm}^{-1}$  is due to the N—H stretching of the —NH—R groups. The appearance of these peaks suggests formation of a crosslinked chitosan/gelatin hybrid polymer network in the composite. Therefore, it can be concluded that incorporation of HA does not disturb the formation of the network. Furthermore, the network not only serves as a matrix to the HA powder, but also provides anchoring of HA powder in the structure, binding them together to form composites.

It is inferred that there are interactions between  $\text{Ca}^{2+}$  and  $\text{PO}_4^{3-}$  groups of HA and between

$\text{COO}^-$  and  $\text{NH}_4^+$  groups of gelatin. In addition, there may be crosslinks between the —OH of HA and the —CHO of glutaraldehyde. Details are under further study.

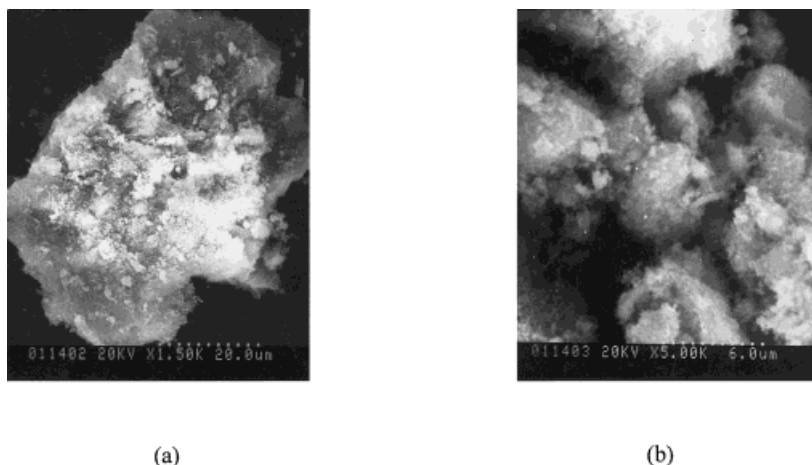
### XRD Analysis

Figure 4 shows XRD patterns of the composite with HA content ranging from 0 to 100% by mass. It can be seen from the patterns that, with an increase in the HA content, the peak centered at  $20.8^\circ$  ( $2\theta$ ), which represents the crystallinity of the polymer, becomes wider and flatter with the peak splitting into many smaller ones. Especially when the HA content reaches 70%, the peak nearly complies with the datum line. This means that the introduction of HA makes the crystallinity of the polymer matrix lower than before. The intervention of HA will weaken the intermolecular interactions, such as H-bonding interactions within the network, while the characteristic peaks of HA gradually become apparent and intensive compared to the peak centered at  $20.8^\circ$  ( $2\theta$ ). Figure 4(c) shows the XRD pattern of the composite with 70% HA, which is practically the same as that of the pure HA [Fig. 4(d)]. Such a result reveals that the organic matrix of the composite has no obvious influence on the crystallinity of HA in our blending method.

### Preparation of Composites

Two processing methods were adopted in preparing the HA/chitosan–gelatin composites. For the first, because the chitosan solution is unusually viscous even at a low concentration ( $<8\text{ wt }%$ ), the incorporated HA powders are much easier to aggregate than to disperse uniformly in the solution. So, the HA powders are dispersed in deionized distilled water using ultrasonication before mingling the slurry attained with the chitosan solution. By this way, the HA powders may remain homogeneously dispersed in the viscous polymer solution. When air-dried, a less uniform end product, which has shrunk considerably, is obtained. The phenomenon is like that found by Wan et al.<sup>18</sup>

In addition, a porous composite can be prepared by a unique sol–gel method. The HA powders are dispersed by copulverizing with other components. Because of the high solid content and the gelation character of the gelatin at ambient ( $<30^\circ\text{C}$ ), the resulting paste appears as a sol state when molded at  $50^\circ\text{C}$ , but turns to a rubbery



**Figure 5** SEM micrographs of (a) original HA powders and (b) pulverized HA powders.

plate at 15°C. By keeping its shape and air-drying simultaneously to thoroughly evaporate the solvent, a porous HA/chitosan-gelatin composite is formed.

### Mechanical Properties

Intimate bonding between HA particles and the organic matrix will improve the mechanical properties of the composites. Thus, to increase the specific area, HA powders were pulverized in advance. Figure 5(a) illustrates the original HA powders, the aggregate characterized by its extremely irregular and rough surface. However, after the pulverization, the aggregate disintegrates to smaller particles with an average size less than 10  $\mu\text{m}$  [Fig. 5(b)]. The composite with pulverized HA exhibits higher mechanical properties than that with the original HA. Data from both composites are summarized in Table II.

Figure 6(a,b) shows the fracture surface of the composites containing (a) the original HA particles and (b) the pulverized ones. Pulverization of HA powders results in differences in the fracture surface morphology of the composites. In Figure 6(a), the HA particle aggregates can clearly be seen and they are only partly surrounded by the organic matrix. Figure 6(b) shows the HA particles embedded in the matrix, and no clear polymer-HA interface can be observed. The morphology gives a good explanation of the increase in the mechanical properties.

### Fracture Texture of the Composites

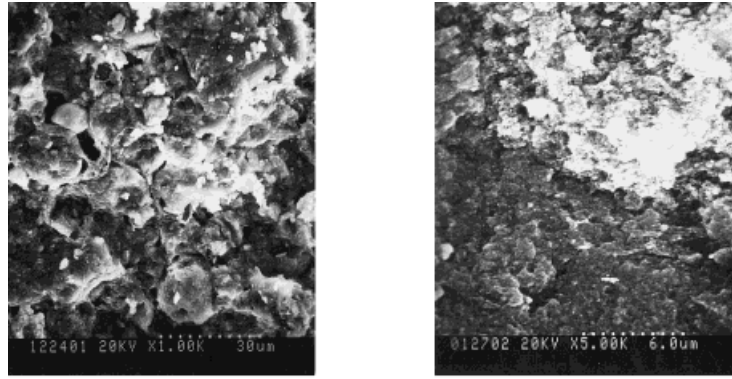
Figure 7 shows SEM micrographs of the fracture surfaces of the resultant composites with differ-

ent HA contents. It can be seen that the fracture surface of the original polymer specimen [Fig. 7(a)] appears level and smooth, while with an increase in the HA content, it becomes rougher and rougher and uneven. Figure 7(b) indicates the jagged surface of the composite with 10 wt % HA. The morphology also exhibits the parallel alignment of the polymer matrix. When the HA content reached 30% [Fig. 7(c)], the alignment becomes more irregular but still can be distinguished. In Figure 7(d), the fracture surface of the composite with 50% HA is full of bumps and hollows with many crystallites randomly distributed inside the polymer matrix. Similar to the results of XRD tests, the changes are also attributed to the weaker intermolecular interactions among the polymer chains in the polymer network. The 100% HA sample shows a coarse surface, which looks loose and very different from those of the composites [Fig. 7(e)].

Figure 8 illustrates the porous structure of the composite with 70% HA prepared by the sol-gel method. The pore-size distribution is in the range of 7–25  $\mu\text{m}$ . Porous networks allow the tissue to

**Table II** Mechanical Properties of Composites with Pure HA (<75  $\mu\text{m}$ ) and Pulverized HA (<10  $\mu\text{m}$ )

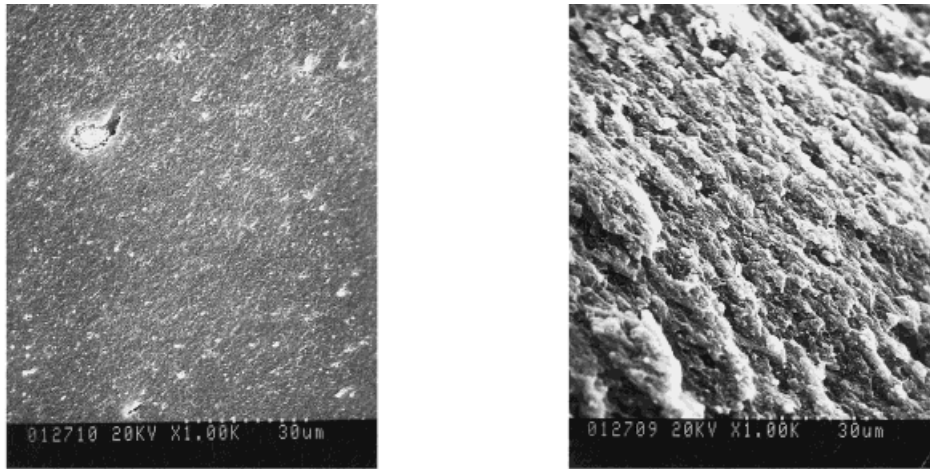
Composite Samples	Impact Strength (kJ/m <sup>2</sup> )	Bending Strength (MPa)
With pure HA	8.38	27
With pulverized HA	11.96	32



(a)

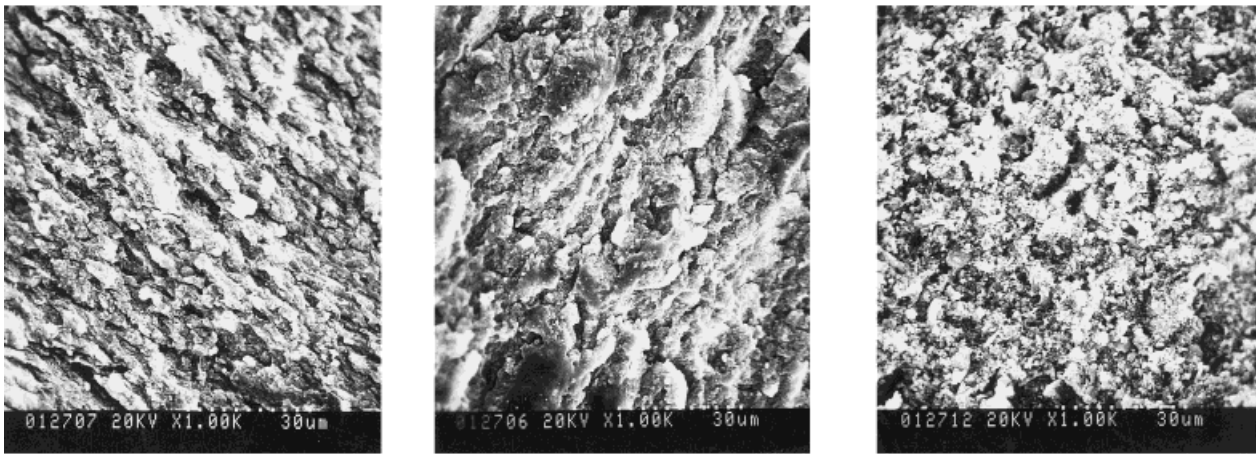
(b)

**Figure 6** (a) Fracture surface of the composites with original HA powders. (b) Fracture surface of the composites with pulverized HA powders.



(a)

(b)



(c)

(d)

(e)

**Figure 7** SEM micrographs of the fracture surfaces of the resultant composites with different HA contents: (a) 0% HA; (b) 10% HA; (c) 30% HA; (d) 50% HA; (f) 100%HA.



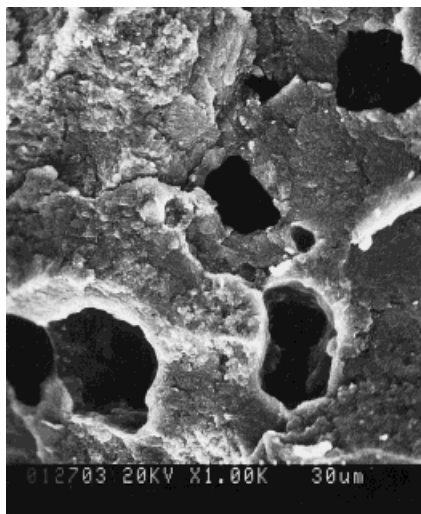


**Figure 8** Fracture surface of a porous composite with 70% HA.

infiltrate, which further enhances the implant-tissue attachment, and the interconnecting porous network may provide advantages for body fluid and blood circulation, with further supply of the nutrients and mineral ions for necessary functional and biological processes. According to some authors,<sup>32,33</sup> for colonization of the pores by bone tissue to take place, the pores must be larger than 50–100  $\mu\text{m}$  or even 250–300  $\mu\text{m}$ . Therefore, the porous structure and resorbable chitosan-gelatin biomimetic matrix are anticipated to benefit the ingrowth of cells, soft tissues, and new bone into the implants. The pore-size distribution and porosity need to be controlled, which is the subject of a following study.

## CONCLUSIONS

In this study, a novel bone-replacing composite composed of HA and the chitosan-gelatin network was developed. IR, SEM, and XRD were applied to study the composite formation and changes in the morphology and crystallinity. The results indicate that the presence of HA does not retard the formation of the chitosan/gelatin network in the composites, while HA still keeps its high crystallinity. A special sol-gel processing method was used to prepare porous composites. The composites with good mechanical properties will provide a promising potential for bone-substitution and bone-remodeling biomedical applications. Studies on its biocompatibility and bio-

degradation properties will be published in the near future.

The authors wish to thank the National Science Foundation of China through Grant No. 59883002 for supporting this research.

## REFERENCES

1. Lin, F. H.; Yao, C. H.; Sun, J. S.; Liu, H. C.; Huang, C. W. *Biomaterials* 1998, 19, 905–917.
2. Willems, G.; Lambrechts, P.; Braem, M.; Vanherle, G. *Quintess Int* 1993, 24, 641–658.
3. Labella, R.; Braden, M.; Deb, S. *Biomaterials* 1994, 15, 1197–1200.
4. Shareef, M. Y.; Messer, P. E. *Biomaterials* 1993, 14, 69–75.
5. Wang, R. Z.; Cui, F. Z.; Lu, H. B.; Wen, H. B.; Ma, C. L.; Li, H. D. *J Mater Sci Lett* 1995, 14, 490–492.
6. Cui, F. A.; Du, C.; Su, X. W.; Zhu, X. D.; Zhao, N. M. *Cells Mater* 1996, 1–3, 31–44.
7. Doi, Y.; Horiguchi, T.; Kim, S. H.; Moriwaki, Y.; Wakamatsu, N.; Adachi, M.; Ibaraki, K.; Moriyama, K.; Sasaki, S.; Shimokawa, H. *Arch Oral Biol* 1992, 37, 15–21.
8. Sugaya, A.; Minabe, M.; Tamura, T.; Hori, T.; Watanabe, Y. *J Periodont Res* 1989, 24, 284–288.
9. Iwano, T.; Kurosawa, H.; Muease, K.; Takeuchi, H.; Ohkubo, Y. *Clin Orthop* 1991, 268, 243–252.
10. Richard, K.; Gongloff, R. K.; Montgomery, C. K. *J Oral Maxillofac Surg* 1985, 43, 845–849.
11. Du, C.; Cui, F. Z.; Feng, Q. L.; Zhu, X. D.; de Groot, K. *J Biomed Mater Res* 1998, 42, 540–548.
12. Kevor, S.; Huisen, T.; Brown, P. W. *J Biomed Mater Res* 1994, 28, 27–33.
13. Bigi, A.; Panzavolta, S. *Roveri Biomater* 1998, 19, 739–744.
14. Sasaki, N.; Umeda, H.; Okada, S.; Kojima, R.; Fukuda, A. *Biomaterials* 1989, 10, 129–132.
15. Ito, M.; Yamagishi, T.; Sugai, T. *J Jpn Soc Dent Mater Devi* 1990, 9, 608–616.
16. Ito, M. *Biomaterials* 1991, 12, 41–45.
17. Kawakami, T.; Antoh, M.; Hasegawa, H.; Yamagishi, T.; Ito, M.; Eda, S. *Biomaterials* 1992, 13, 759–763.
18. Wan, A. C. A.; Khor, E.; Hastings, G. W. *J Biomed Mater Res Appl Biomater* 1998, 38, 235–241.
19. Liu, Q.; Wijn, J. R.; Blitterswijk, C. A. *J Biomed Mater Res* 1998, 40, 490–497.
20. Doyle, C.; Tanner, K. E.; Bonfield, W. *Biomaterials* 1991, 12, 841–847.
21. Higashi, S.; Yamamuro, T.; Nakamura, T.; Ikada, Y.; Hyon, S. H.; Jamshidi, K. *Biomaterials* 1986, 7, 183–187.
22. Ignjatovic, N.; Tomic, S.; Dakic, M.; Miljkovic, M.; Plavsic, M.; Uskokovic, D. *Biomaterials* 1999, 20, 809–816.

23. Zhang, R.; Ma, P. X. *J Biomed Mater Res* 1999, 44, 446–455.
24. Yao, C. H.; Sun, J. S.; Lin, F. H.; Liaw, J. R.; Huang, C. W. *Mater Chem Phys* 1996, 45, 6–14.
25. Hunter, G. K.; Nyburg, S. C.; Pritzker, K. P. H. *Coll Rel Res* 1986, 6, 229–238.
26. Brecevic, L.; Hlady, V.; Milhofer, H. F. *Coll Surf* 1987, 28, 301–313.
27. Hoppe-Seiler, F. *Ber Deutsch Chem Ges* 1994, 27, 3329–3331.
28. Rao, B. S.; Sharma, C. P. *J Biomed Mater Res* 1997, 34, 21–28.
29. Hirano, S.; Noishiki, Y. *J Biomed Mater Res* 1985, 19, 413–417.
30. Ito, M.; Yamagishi, T.; Yagasaki, H.; Kafrawy, A. H. *J Biomed Mater Res* 1996, 32, 95–98.
31. Ito, M.; Hidaka, Y.; Nakajima, M.; Yagasaki, H.; Kafrawy, A. H. *J Biomed Mater Res* 1999, 45, 204–208.
32. Klawiter, J. J.; Bagwell, J. G.; Weinstein, A. M.; Sauer, B. W.; Pruitt, J. R. *J Biomed Mater Res* 1976, 10, 311–321.
33. Daculsi, G.; Passuti, N. *Biomaterials* 1990, 11, 86–87.